MESOSPHERIC CARBON DIOXIDE AND TEMPERATURE RETRIEVALS FROM NOMAD-SO ONBOARD TGO.

L. Trompet, A.C. Vandaele, I. Thomas *Royal Belgian Institute for Space Aeronomy, Brussels, Belgium (loic.trompet@aeronomie.be)*, **S. Aoki** *Graduate School of Frontier Sciences, The University of Tokyo, Kashiwa, Japan*, **F. Daerden, J. Erwin, Z. Flimon, A. Mahieux, L. Neary, S. Robert** *Royal Belgian Institute for Space Aeronomy, Brussels, Belgium*, **G. Villanueva, G. Liuzzi** *Goddard Flight Space Center, GFSC, Greenbelt, USA*, **M.A. Lopez-Valverde, A. Brines, J. J. Lopez-Moreno** *Instituto de Astrofisica de Andalucia, IAA/CSIC, Spain*, **G. Bellucci** *Istituto di Astrofisica e Planetologia Spaziali, IAPS/INAF, Rome, Italy*, **M. R. Patel** [8]*School of Physical Sciences, The Open University, Milton Keynes, UK.*

Introduction:

Mars mesosphere is the place of many atmospheric phenomena such as gravity waves, large amplitudes tides and temperature inversion. The mesosphere has been less studied than the lowest and highest altitudes but NOMAD-SO (SO in the following) is regularly scanning the Mars atmosphere from the troposphere to an altitude around 200 km and we focus in this work on the retrievals in the mesosphere.

The SO channel of the NOMAD instrument (Vandaele et al., 2015) is dedicated to solar occultation measurements and the derived profiles are located at the terminator. SO is an infrared spectrometer (2.3-4.3 µm) composed of an echelle grating with an acousto-optical tunable filter for diffraction order selection. In this work, we focus on the retrievals from diffraction order 148 which is centered on the CO_2 fundamental band 21102-00001 (AFGL code) and covers the spectral range 3325.6 cm^{-1} to 3351.9 cm^{-1}. We derived 963 profiles from the full Martian years (MY) 35 and from MY 36 until a solar longitude (Ls) of 135° (23/03/2019 till 01/12/2021). The latitude covered by this dataset are located mainly around 60° North and 60° South with still some profiles located closer to the equator (see Figure 2, the blue points represent all measurements for this dataset).

Method:

The retrieval method is split into three main steps. First, slant columns are inverted for each SO spectrum individually with the ASIMUT radiative transfer code (Vandaele et al., 2006) based on the optimal estimation method (Rodgers, 2000). The highest altitude bound is limited by the strength of the CO_2 lines and the lowest one by the saturation of the CO_2 lines.

The second step is the vertical inversion. The slant column profile is converted into a vertical density profile with an iterated Tikhonov method (Quémerais et al., 2006). This method requires providing a regularization parameter. With a synthetic example, we tested 7 methods to infer the best regularization method and the best one appears to be the expected error estimation (Doicu et al., 2010; Xu et al., 2016).

In the third step, we derive the pressure and temperature profiles with the hydrostatic equilibrium equation (Mahieux, 2011; Snowden et al., 2013). This step is usually performed numerically but we derived an analytical formula that makes the error computation easier. The uncertainties are on average 10 K at 0.02 Pa (around 90 km) and 2 K at 0.4 Pa (around 60 km).

Results:

Figure 1 shows the retrieved carbon dioxide density values at 75 km. As expected, we see lower values near aphelion and highest values close to perihelion. We also see that, closer to aphelion, the values in the Southern hemisphere are lower than in the Northern hemisphere. The inverse happens closer to perihelion.

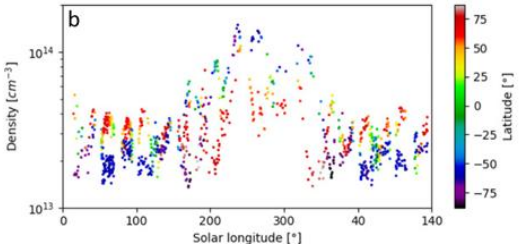

Figure 1: Carbon dioxide density at 75 km retrieved from NOMAD-SO during MY 35 and the beginning of MY 36.

The temperature profiles show several warm layers mainly appearing at dawn in both hemispheres and dusk in the Northern hemisphere while they are more homogeneous at Southern dusks between Ls 50° and 150°. The location of the warm layers at the beginning of MY 35 and 36 are very similar.

We compare our results with MRO-MCS (Zurek & Smrekar, 2007; Kleinböhl et al., 2009) co-located profiles. They are in good agreement with an average difference of 3 K. The main differences can be explained by a difference in location.

We also compared our results to those of the GEM-Mars GCM (Neary & Daerden, 2018; Daerden et al., 2019, 2022) interpolated for the location of SO profiles. The profiles agree well except for the presence in SO profiles of a colder layer in the Southern hemisphere for the beginning of the year (until Ls 60°), a warmer layer at Ls 300° to 360° and a warm layer at dawn in the Northern hemisphere for Ls 240° to

360°.

Figure 1 shows some examples of SO temperature profiles that have very close latitude, local time and Ls but different longitudes. The upper panel contains profiles at dawn and the lower panel contains profiles at dusk. We see more variability and even some strong temperature inversion between 55 and 70 km for the profiles at dawn and more monotonic profiles at dusk.

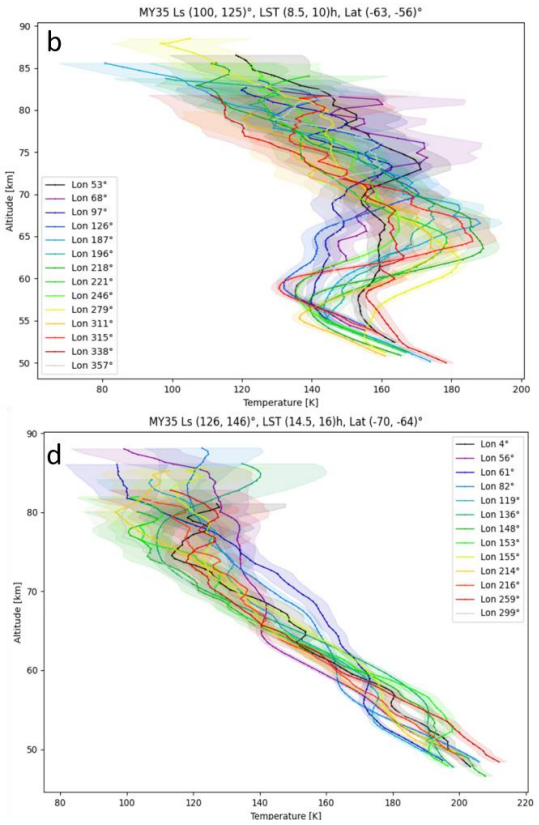

Figure1: Two examples of SO temperature profiles. The locations are given above the panels. Panel b for dawn and panel d for dusk.

To the temperature, we fitted the formula $A\ cos(k\ \lambda - \varphi)$ where k is the wavenumber (1, 2, 3 or 4), λ is the longitude, A is the amplitude and φ is the phase. In the case at dawn (panel a), we derived a wavenumber-1 component with an amplitude of 10% of the background temperature and with still a remaining wavenumber-3 component of 5%.

We also checked the presence of a strong warm layer with a method similar to Nakagawa et al. (2020). Their presence is given in orange and green in Figure 2. The warm layers are present in 20% of the dataset, mainly in the morning around 9 h and in the Southern hemisphere for the first half-year and in the Northern hemisphere in the second half-year.

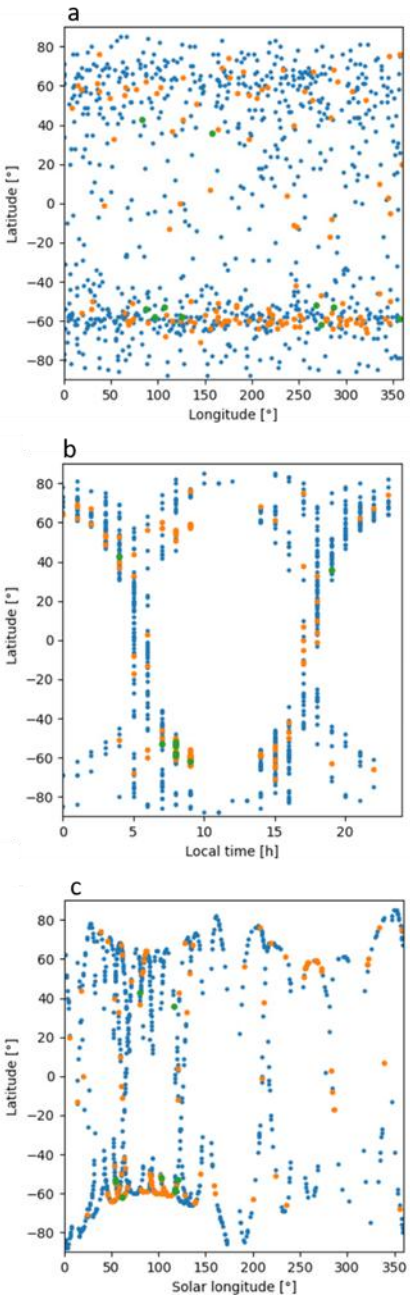

Figure2: In blue: location of all profiles for diffraction order 148 in MY35 and 36 until Ls 135°. In orange: location of profiles with a warm layer. In green: location of profiles with two warm layer.

We also report that amongst the 963 profiles, six of them contain some values lower than the temperature limit for CO_2 condensation. Those profiles are presented in Figure 3. Two of them were already reported in Liuzzi et al. (2021). Those six profiles are located at places where CO_2 ice clouds were already reported except for the one at Ls 213° (red in Figure 3).

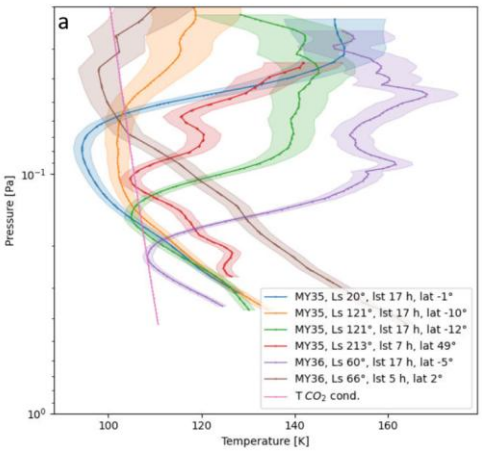

Figure 3: Six temperature profiles with a value lower than the temperature limit for CO_2 condensation.

Conclusions:

We derived 963 CO_2 and temperature profiles of the mesosphere of Mars. Many of those temperature profiles contain specific features. The temperature profiles retrieved for the beginning of MY35 and MY36 show the same latitudinal trends. The seasonal variations show similar behavior to previous studies and simulations (see for instance, Forget et al., 2009; González-Galindo et al., 2011). Some clear longitudinal trends are visible in the profiles at high latitudes around 60°. We derived the longitudinal components. Some strong warm layers were already reported on the night side and we report their presence as well at the terminator in 20% of the profiles. We also report the presence of six temperature profiles with a temperature lower than the temperature limit for CO_2 condensation. Those results have been submitted in two papers (Trompet et al., 2022; Trompet, et al., 2022) and another analysis on MY34 Ls 160 to 360° has been submitted in (Lopez-Valverde et al., 2022)

Acknowledgement:

The NOMAD experiment is led by the Royal Belgian Institute for Space Aeronomy (IASB-BIRA), assisted by Co-PI teams from Spain (IAA-CSIC), Italy (INAF-IAPS), and the United Kingdom (Open University). This project acknowledges funding by the Belgian Science Policy Office (BELSPO), with the financial and contractual coordination by the ESA Prodex Office (PEA 4000103401, 4000121493), by the Spanish Ministry of Science and Innovation (MCIU), and by European funds under grants PGC2018-101836-B-I00 and ESP2017-87143-R (MINECO/FEDER), as well as by UK Space Agency through grants ST/V002295/1, ST/V005332/1, and ST/S00145X/1 and Italian Space Agency through grant 2018-2-HH.0. This work was supported by the Belgian Fonds de la Recherche Scientifique – FNRS under grant number 30442502 (ET_HOME). This project has received funding from the European Union's Horizon 2020 research and innovation program under grant agreement No 101004052 (RoadMap project). The IAA/CSIC team acknowledges financial support from the State Agency for Research of the Spanish MCIU through the 'Center of Excellence Severo Ochoa' award for the Instituto de Astrofísica de Andalucía (SEV-2017-0709) and funding by grant PGC2018-101836-B-100 (MCIU/AEI/FEDER, EU). US investigators were supported by the National Aeronautics and Space Administration. Canadian investigators were supported by the Canadian Space Agency.

References:

Daerden, F., Neary, L., Villanueva, G., Liuzzi, G., Aoki, S., Clancy, R. T., Whiteway, J. A., Sandor, B. J., Smith, M. D., Wolff, M. J., Pankine, A., Khayat, A., Novak, R., Cantor, B., Crismani, M., Mumma, M. J., Viscardy, S., Erwin, J., Depiesse, C., … Vandaele, A. C. (2022). Explaining NOMAD D/H Observations by Cloud-induced Fractionation of Water Vapor on Mars. *Journal of Geophysical Research: Planets*, *127*(2), e2021JE007079. https://doi.org/10.1029/2021JE007079

Daerden, F., Neary, L., Viscardy, S., García Muñoz, A., Clancy, R. T., Smith, M. D., Encrenaz, T., & Fedorova, A. (2019). Mars atmospheric chemistry simulations with the GEM-Mars general circulation model. *Icarus*, *326*, 197–224. https://doi.org/10.1016/j.icarus.2019.02.030

Doicu, A., Trautmann, T., & Schreier, F. (2010). Numerical Regularization for Atmospheric Inverse Problems. In *Numerical Regularization for Atmospheric Inverse Problems*. Springer Berlin Heidelberg. https://doi.org/10.1007/978-3-642-05439-6

Forget, F., Montmessin, F., Bertaux, J. L., González-Galindo, F., Lebonnois, S., Quémerais, E., Reberac, A., Dimarellis, E., & López-Valverde, M. A. (2009). Density and temperatures of the upper Martian atmosphere measured by stellar occultations with Mars Express SPICAM. *Journal of Geophysical Research E: Planets*, *114*(1), 1004. https://doi.org/10.1029/2008JE003086

González-Galindo, F., Määttänen, A., Forget, F., & Spiga, A. (2011). The martian mesosphere as revealed by CO2 cloud observations and General Circulation Modeling. *Icarus*, *216*(1), 10–22. https://doi.org/10.1016/J.ICARUS.2011.08.006

Kleinböhl, A., Schofield, J. T., Kass, D. M., Abdou, W. A., Backus, C. R., Sen, B., Shirley, J. H., Lawson, W. G., Richardson, M. I., Taylor, F. W., Teanby, N. A., & McCleese, D. J. (2009). Mars Climate Sounder limb profile retrieval of atmospheric temperature, pressure, and dust and water ice opacity. *Journal of Geophysical Research E: Planets*, *114*(10), 1–30. https://doi.org/10.1029/2009JE003358

Liuzzi, G., Villanueva, G. L., Trompet, L., Crismani, M. M. J., Piccialli, A., Aoki, S., Lopez- Valverde, M. A., Stolzenbach, A., Daerden, F., Neary, L., Smith, M. D., Patel, M. R., Lewis, S. R., Clancy, R. T., Thomas, I. R., Ristic, B., Bellucci, G., Lopez- Moreno, J., & Vandaele, A. C. (2021). First Detection and Thermal Characterization of Terminator CO 2 Ice Clouds with ExoMars/NOMAD. *Geophysical Research Letters*, *48*(22), e2021GL095895. https://doi.org/10.1029/2021gl095895

Lopez-Valverde, M.-A., Funke, B., Brines, A., Stolzenbach, A., Modak, A., Hill, B., Francisco, G.-G., Thomas, I., Trompet, L., Aoki, S., Villanueva,

G., Liuzzi, G., Erwin, J., Vandaele, A.-C., Grabowski, U., Forget, F., Moreno, J. J. L., Rodriguez, J., Ristic, B., … Patel, M. (2022). Martian atmospheric temperature and density profiles during the 1st year of NOMAD/TGO solar occultation measurements. *Journal of Geophysical Research: Planets, Submitted*.

Mahieux, A. (2011). *Inversion of the infrared spectra recorded by the SOIR instrument on board VenusExpress* [Université Libre de Bruxelles]. http://planetary.aeronomie.be/multimedia/pdf/These_ArnaudMahieux_2011.pdf

Nakagawa, H., Jain, S. K., Schneider, N. M., Montmessin, F., Yelle, R. V., Jiang, F., Verdier, L., Kuroda, T., Yoshida, N., Fujiwara, H., Imamura, T., Terada, N., Terada, K., Seki, K., Gröller, H., & Deighan, J. I. (2020). A Warm Layer in the Nightside Mesosphere of Mars. *Geophysical Research Letters*, *47*(4), 1–10. https://doi.org/10.1029/2019GL085646

Neary, L., & Daerden, F. (2018). The GEM-Mars general circulation model for Mars: Description and evaluation. *Icarus*, *300*, 458–476. https://doi.org/10.1016/j.icarus.2017.09.028

Quémerais, E., Bertaux, J. L., Korablev, O., Dimarellis, E., Cot, C., Sandel, B. R., & Fussen, D. (2006). Stellar occultations observed by SPICAM on Mars Express. *Journal of Geophysical Research E: Planets*, *111*(9), 9–13. https://doi.org/10.1029/2005JE002604

Rodgers, C. D. (2000). *Inverse methods for atmospheric sounding* (Vol. 2). WORLD SCIENTIFIC. https://doi.org/10.1142/3171

Snowden, D., Yelle, R. V., Cui, J., Wahlund, J.-E. E., Edberg, N. J. T. T., & Ågren, K. (2013). The thermal structure of titan's upper atmosphere, I: Temperature profiles from Cassini INMS observations. *Icarus*, *226*(1), 552–582. https://doi.org/10.1029/2010JA016251

Trompet, L., Vandaele, A. C., Thomas, I., Aoki, S., Daerden, F., Erwin, J., Flimon, Z., Mahieux, A., Neary, L., Robert, S., Villanueva, G., G. Liuzzi, 6, Lopez-Valverde, M. A., Brines, A., Bellucci, G., Lopez-Moreno, J. J., & Patel, M. R. (2022). Carbon dioxide retrievals from NOMAD-SO on ESA's ExoMars Trace Gas Orbiter and temperature profiles retrievals with the hydrostatic equilibrium equation. II. Temperature variabilities in the mesosphere at Mars terminator. *Journal of Geophysical Research: Planets, Submitted*.

Trompet, L., Vandaele, A. C., Thomas, I., Aoki, S., Daerden, F., Erwin, J., Flimon, Z., Mahieux, A., Neary, L., Robert, S., Villanueva, G., Liuzzi, G., Lopez-Valverde, M. A., Brines, A., Bellucci, G., Lopez-Moreno, J. J., & Patel, M. R. (2022). Carbon dioxide retrievals from NOMAD-SO on ESA's ExoMars Trace Gas Orbiter and temperature profiles retrievals with the hydrostatic equilibrium equation. I. Description of the method. *Journal of Geophysical Research: Planets, Submitted*.

Vandaele, A. C., Kruglanski, M., & De Mazière, M. (2006). Modeling and retrieval of atmospheric spectra using ASIMUT. *European Space Agency, (Special Publication) ESA SP*, *618*.

Vandaele, A. C., Neefs, E., Drummond, R., Thomas, I. R. R., Daerden, F., Lopez-Moreno, J.-J. J., Rodriguez, J., Patel, M. R. R., Bellucci, G., Allen, M., Altieri, F., Bolsée, D., Clancy, T., Delanoye, S., Depiesse, C., Cloutis, E., Fedorova, A., Formisano, V., Funke, B., … Wolff, M. (2015). Science objectives and performances of NOMAD, a spectrometer suite for the ExoMars TGO mission. *Planetary and Space Science*, *119*, 233–249. https://doi.org/10.1016/j.pss.2015.10.003

Xu, J., Schreier, F., Doicu, A., & Trautmann, T. (2016). Assessment of Tikhonov-type regularization methods for solving atmospheric inverse problems. *Journal of Quantitative Spectroscopy and Radiative Transfer*, *184*, 274–286. https://doi.org/10.1016/j.jqsrt.2016.08.003

Zurek, R. W., & Smrekar, S. E. (2007). An overview of the Mars Reconnaissance Orbiter (MRO) science mission. In *Journal of Geophysical Research E: Planets* (Vol. 112, Issue 5, pp. 5–6). John Wiley & Sons, Ltd. https://doi.org/10.1029/2006JE002701